Available online at www.sciencedirect.com
SCIENCE DIRECT®
Nuclear Instruments and Methods in Physics Research B 242 (2006) 1–7
NIM B
Beam Interactions with Materials & Atoms
www.elsevier.com/locate/nimb

Bioactivity of plasma implanted biomaterials

Paul K. Chu *

Department of Physics and Materials Science, City University of Hong Kong, Tat Chee Avenue, Kowloon, Hong Kong

Available online 12 September 2005

Abstract

Plasma immersion ion implantation and deposition (PIII&D) is an effective technique to enhance the surface bioactivity of materials. In this paper, recent progress made in our laboratory on plasma surface modification of biomedical materials is described. NiTi alloys have unique super-elastic and shape memory properties and are suitable for orthopedic implants but the leaching of toxic Ni may pose health hazards in humans. We have recently investigated the use of acetylene, oxygen and nitrogen PIII&D to prevent out-diffusion of nickel and good results have been obtained. Silicon is the most important material in the microelectronics industry but its surface biocompatibility has not been investigated in details. We have recently performed hydrogen PIII into silicon to improve the surface bioactivity and observed biomimetic growth of apatite on the surface in simulated body fluids. Diamond-like carbon (DLC) is widely used in the industry due to its excellent mechanical properties and chemical inertness and by incorporation of elements such as nitrogen and phosphorus, the surface blood compatibility can be improved. The properties as well as in vitro biological test results are discussed in this article.

PACS: 52.75.R; 52.65.R; 52.65.C; 61.72.T

Keywords: NiTi shape memory alloys; Plasma implantation; Bioactivity; Apatite; Amorphous carbon; Blood compatibility; Silicon

1. Introduction

The use of plasma immersion ion implantation and deposition (PIII&D) to enhance the surface bioactivity of materials has attracted much interest [1–4]. In this paper, our recent work on plasma surface modification of orthopedic NiTi shape memory alloys to mitigate the out-diffusion of toxic nickel, improvement of surface bioactivity of single-crystal silicon using hydrogen PIII, as well as the enhancement of the surface blood compatibility of amorphous carbon thin films via implantation of nitrogen and phosphorus is described.

2. Nickel–titanium orthopedic alloys

Nickel–titanium (NiTi) shape memory alloys are promising materials for surgical implants in orthopedics due to their unique shape memory effect and super-elasticity that most metallic biomaterials such as stainless steels and titanium alloys do not possess. In addition, their mechanical properties are closer to those of cortical bones than stainless steels and titanium alloys. However, some negative side effects have been pointed out [5]. For example, the osteogenesis process and osteonectin synthesis activity in NiTi alloys are unfavorable compared to stainless steels and titanium alloys [6], the cell death rate is severe on NiTi alloys [7] and proliferation of human gingival fibroblasts on NiTi samples with rough surface is slow compared to stainless steels and Ti alloys with the same surface roughness [8]. These problems are believed to stem from the poor corrosion resistance of the materials thereby lead to an increase of the cytotoxicity. Other studies have also reported that nickel ions [9,10] leached from the alloys cause toxic reactions in humans, more severely in nickel hyper-sensitive patients resulting in strong allergic reactions [11–14]. Therefore, it is important to enhance the corrosion resistance and anti-wear properties of the materials before the materials can

* Tel.: +852 2788 7724; fax: +852 2788 9549/2788 7830.
E-mail address: paul.chu@cityu.edu.hk

0168-583X/$ - see front matter © 2005 Elsevier B.V. All rights reserved.
doi:10.1016/j.nimb.2005.08.015

be more widely used clinically, especially as orthopedic implants with couplings where fretting is expected.

Since the leaching out of harmful Ni ions to body issues and fluids inside the human body has been raising much safety concern, we therefore aim at producing barrier layers to impede the out-diffusion of Ni ions. The technique used here is plasma immersion ion implantation and deposition (PIII&D) [1,15–17] and three different gas plasmas, C_2H_2, N_2 and O_2, are used. The implant fluence is typically about 10^{17} cm^{-2} and implantation voltage is between 20 and 40 kV. The PIII&D treatment is performed without external heating and the sample temperature is typically below 200 °C. Titanium carbides and nitrides possess excellent mechanical and chemical properties such as high hardness, low wear coefficient and chemical inertness [18–21] whereas titanium oxides have very good biocompatibility [22–26] and also chemical stability. Both titanium oxides and nitrides films have been formed by coating or implantation into NiTi substrates by different means. It should be noted that due to favorable ion mixing effects in PIII&D, no discrete interface results and layer delamination is much reduced.

In addition to performing corrosion tests [27,28], the treated and control samples are immersed in 25 ml of simulated body fluids (SBF) in polypropylene (pp) bottles at 37 ± 0.1 °C for five weeks. After five weeks, the SBF in the bottles are analyzed by inductively-coupled plasma mass spectrometry (ICPMS) to determine the amounts of Ni and Ti leached from each specimen. The dissolution test results in Table 1 shows that the amount of Ni leached out from the control sample is 24–35 times that of the treated samples. Thus, the modified surface layer is evidently effective in mitigating the out-diffusion of Ni from the substrate.

Our results indicate that the amount of Ni that leaches out from the bulk is reduced to low levels in all three types of PIII samples. This may be ascribed to the higher affinity of Ti towards C, N and O to form chemical bonds than Ni thus providing a driving force to enrich the surface with the element forming a stronger chemical bond and so Ni is segregated away from the surface. The heat of formation of the lowest titanium oxide is -913 kJ mol^{-1} while that of NiO is -244 kJ mol^{-1} [29]. The heat of formation of TiN is -305.6 kJ mol^{-1} [30], whereas nickel nitrides such as Ni_3N are unstable compared to TiN [31]. The heat of formation of TiC is -773 kJ mol^{-1} [32] while that of NiC is not well established because the Ni–C phase diagram does not show stable carbides. The term nickel carbide may only stand for interstitial solid solutions of C in Ni possessing the NaCl structure [33]. Hence, the formation of titanium oxide, nitride and carbide are energetically favored over those of nickel and this is believed to account for the suppression of surface Ni.

Table 1
Ni concentrations determined by ICPMS in SBF immersion tests

Sample	Ni concentration in SBF (ppb)
Untreated NiTi control	865
C_2H_2-PIII NiTi	24.4
N-PIII NiTi	31.2
O-PIII NiTi	36.2

Our nano-indentation results also reveal that the hardness of the PIII samples is better than the untreated materials and therefore the treated materials are mechanically sturdy [27]. Thus, the structures produced by acetylene, nitrogen and oxygen PIII possess significantly better surface barrier capability against Ni and exhibit very good corrosion resistance and surface mechanical properties.

3. Surface bioactivity of hydrogen plasma implanted silicon

Since the discovery of SiO_2-based bioglass in 1969 [34], possible applications of silicon-containing materials such as wollastonite, silica gel and porous silicon to biomedical engineering have been investigated [35–38]. Silicon is generally considered to be nonessential in biochemistry, except in certain primitive organisms like diatoms [39]. However, silicon has gradually been shown to be an essential trace element in the normal metabolism of higher animals and silicon is required in the formation of bones, cartilages and connective tissues and several important metabolic processes [40]. Modern genetic engineering techniques have been used to demonstrate that certain genes are activated by hydrated silicon [41]. Hydrated soluble silicon has been found to enhance the proliferation of bone cells (osteoblasts) and active cellular production of transforming growth factors [42]. In addition, it has been shown that the critical concentration of ionic products dissolved from the bioactive glass composed of soluble silicon and calcium ions can enhance osteogenesis through the direct control over genes that regulate cell cycle induction and progression [43,44].

Hydrogen in silicon has been widely investigated in the semiconductor industry. For instance, hydrogen alters the electrical properties of microelectronic devices by passivating shallow-level and deep-level defects [45]. It has also been reported that high dose implantation of hydrogen and subsequent annealing induce splitting of Si, a technique used in the fabrication of silicon on insulator (SOI) materials [46]. As a result, a large amount of literature reporting the structure and properties of hydrogen in silicon can be found [47–51], but very little work has been conducted to investigate the role of hydrogen in silicon in biological applications. The only piece of work we have been able to find in the literature reports that the surface functionalization of amorphous hydrogenated silicon (a-Si:H) and amorphous silicon suboxide films (a-SiO_x:H) by hydrosilylation reactions is largely biocompatible [52]. The application of hydrogenated silicon to improve the bioactivity or bone conductivity of silicon has pretty much been unexplored, but the materials have exciting implications in biomedical engineering and biosensor technologies because silicon-based devices often suffer from problems associated with interfacing to the biological environment.

We have recently conducted hydrogen plasma immersion ion implantation (PIII) into single-crystal silicon wafers and observed improved biomimetic growth of apatite on the surface in simulated body fluids [53]. The concept of utilizing Si itself as a bioactive miniaturizable packaging material may thus provide a solution to some of these problems.

In our investigation, hydrogen is plasma implanted into the polished side of ⟨100⟩ silicon wafers using plasma immersion ion implantation (PIII) in the plasma laboratory of the City University of Hong Kong [54,55]. Previous results have shown that under these conditions in our instrument, H_3^+ is the dominated ion species in the plasma [56]. After ultrasonically washed in acetone and rinsed in deionized water, the silicon wafers prior to and after hydrogen implanted are soaked in a simulated body fluid (SBF) buffered at pH 7.4 with trimethanol aminomethane–HCl for 14 and 28 days. The AFM images acquired from the hydrogen-implanted silicon wafer indicate that the surface of the hydrogen-implanted silicon wafer is quite smooth with a root mean square (RMS) roughness of about 0.235 nm which is similar to the roughness of the silicon wafer before hydrogen implantation. Cross-sectional TEM micrograph of the hydrogen-implanted silicon wafer shows the existence of a top amorphous zone about 60 nm in thickness and a 150 nm dense dislocation zone [53].

Figs. 1 and 2 depict the surface views of the un-implanted and hydrogen-implanted samples after soaking in a simulated body fluid (SBF) for 14 and 28 days. After 14 days immersion in the simulated body fluid, the surface of un-implanted silicon wafer remains smooth similar to that of a silicon wafer before immersion (Fig. 1(a)), while some single and clustered ball-shape particles emerge on the hydrogen-implanted silicon surface (Fig. 2(a)). The surface of silicon wafer is, however, not covered completely. The higher magnification micrograph indicates that they have a coral-like structure composed of many sheet-like crystallites (Fig. 2(c)). After an immersion time of 28 days, the surface is entirely covered by the newly formed layer (Fig. 2(b)). In contrast, no new substance can be found on the surface of the un-implanted silicon wafer even after soaking in SBF for 28 days (Fig. 1(b)). In our X-ray fluorescence (XRF) analysis, calcium and phosphorus cannot be detected on the surface of the un-implanted silicon wafer after soaking for 14 and 28 days. However, the XRF spectra acquired from the hydrogen-implanted silicon wafer soaked in SBF for 14 days reveal the existence of surface calcium and phosphorus. After immersion for 28 days, more calcium and phosphorus are detected indicating the formation of a denser and thicker Ca–P layer. The atomic ratios of Ca to P calculated from the XRF results acquired from the hydrogen-implanted silicon soaked in SBF for 14 and 28 days are about 1.33 and 1.58, respectively. Our data show that the atomic ratio of Ca to P in the Ca–P layer increases gradually to that of hydroxyapatite (1.67) with longer immersion time. This indicates that the Ca–P layer formed on the hydrogen-implanted silicon can crystallize to form hydroxyapatite.

Based on our X-ray diffraction results (not shown here), only crystalline silicon peaks are observed whereas no crystalline apatite peaks appear in the XRD patterns obtained from the un-implanted silicon wafers soaked for 14 days and 28 days. The XRD pattern of the hydrogen-implanted silicon wafer soaked in SBF for 28 days shows an obvious difference. The peaks corresponding to crystalline apatite can be easily identified indicating the formation of a new surface layer composed of crystalline apatite and broadening of the peaks suggests that the apatite particles formed on the hydrogen-implanted silicon wafer are superfine or have low crystallinity. Hence, our results reveal the enhancement of surface bioactivity after hydrogen PIII. In order to investigate clearly the formation mechanism of bone-like apatite on the surface of the hydrogen-implanted silicon wafer, two comparative experiments are also conducted. One is to investigate the bioactivity of hydrogenated silicon wafer with no surface damage and the other one is to evaluate the bioactivity of argon implanted silicon wafer which possesses an amorphous surface but no hydrogen. In our experiments, after the hydrogenated silicon wafer and argon implanted wafer are soaked for 28 days, no apatite can be found on either surface suggesting poor bioactivity. It thus appears that

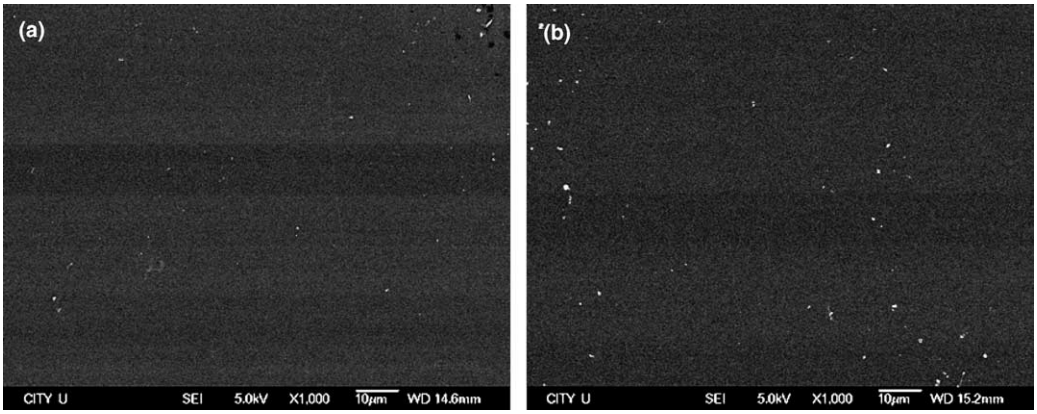

Fig. 1. SEM micrographs of silicon wafer soaked in SBF for (a) 14 days and (b) 28 days.

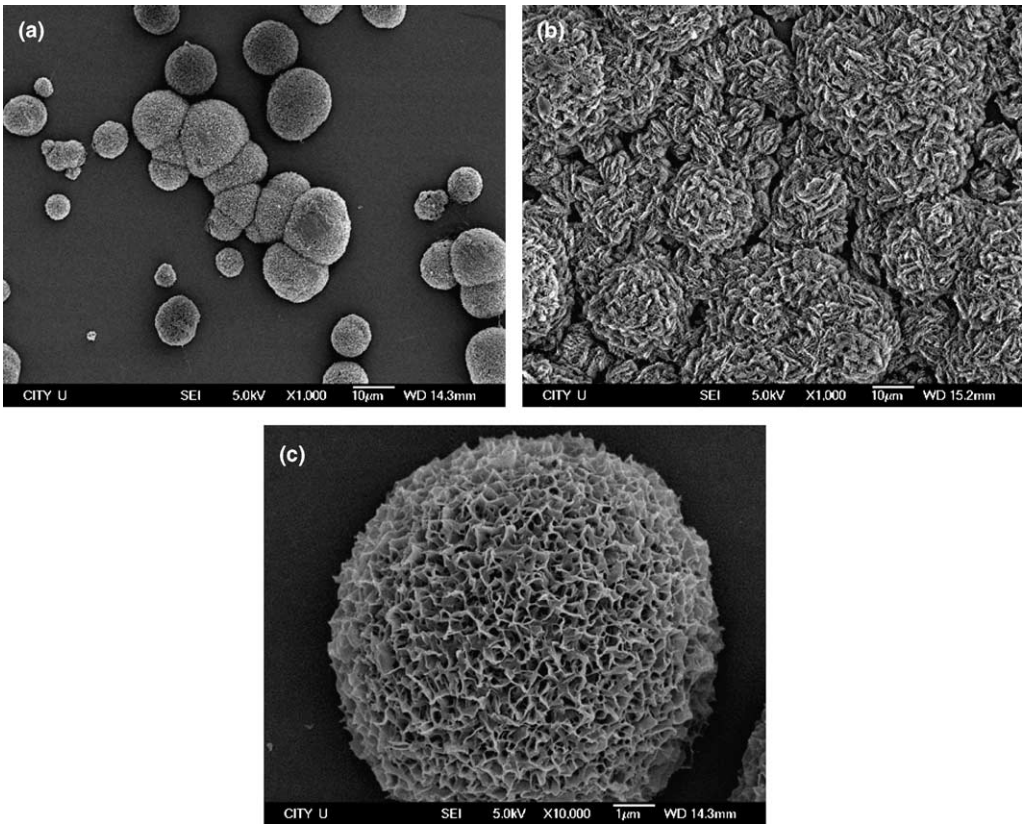

Fig. 2. SEM micrographs of hydrogen-implanted silicon wafer soaked in SBF for: (a) 14 days, (b) 28 days and (c) the higher magnification of the ball-like particles in (a).

only the formation of an amorphous hydrogenated silicon (a-Si:H_x) surface can improve the bioactivity of silicon wafer and experimental evidence has so far suggested that the formation of apatite requires that the surface be both amorphous and hydrogenated.

4. Biocompatibility of doped diamond-like carbon

When natural heart valves undergo degenerative processes such as calcification of leaflets due to infection, aging, or dietary problems, artificial heart valve replacement is a solution and low temperature isotropic pyrolytic carbon (LTIC) is the most common and widely used material. Unfortunately, its blood compatibility is still not adequate and as a result, patients must continue to take blood anti-coagulation medicine [57]. Amorphous carbon (a-C) or diamond-like carbon (DLC) films are potential biomedical materials due to their chemical inertness and excellent mechanical properties [58–60]. Previous studies have shown that amorphous hydrogenated carbon (a-C:H) and DLC thin films with the proper sp^3/sp^2 ratio exhibit good blood compatibility [61–65]. Hydrogen-free DLC or tetrahedral amorphous carbon (ta-C) films [66–68] have attracted considerable interest due to their favorable properties such as superior mechanical properties and chemical resistance compared to a-C:H films, even though biocompatibility studies such as blood compatibility have been quite limited [69]. Plasma surface modification has been shown to be an effective technique to alter the surface biocompatibility and doping amorphous carbon films with a biological friendly element is projected to improve the surface bioactivity. We have thus investigated the addition of nitrogen and phosphorus into DLC using PIII&D to enhance the surface blood compatibility of the materials [70,71].

In our nitrogen doping experiments, both the fabrication of the carbon films and implantation of N are carried out in the same PIII&D machine. Carbon ions are introduced into the chamber by means of a cathodic arc plasma source via a curved magnetic duct that is intended to eliminate macro-particles. The amorphous carbon films produced here are such hydrogen-free. Argon and nitrogen gases are subsequently simultaneously bled into the chamber using separate flow meters to control their individual flow rates. The blood compatibility behavior of the films is evaluated utilizing in vitro platelet adhesion tests. In order to investigate the platelets interaction with the film, the platelet rich plasma (PRP) is employed. It is extracted from human blood by centrifuging for 15 min at 1000 rpm. The samples are immersed into this solution and after rinsing, fixing and critical point drying, the adherent platelets on the sample surface are examined using optical microscopy (OM) and scanning electron microscopy (SEM). Surface thrombogenicity is indicated by the morphology change or activation of the adhesive platelets,

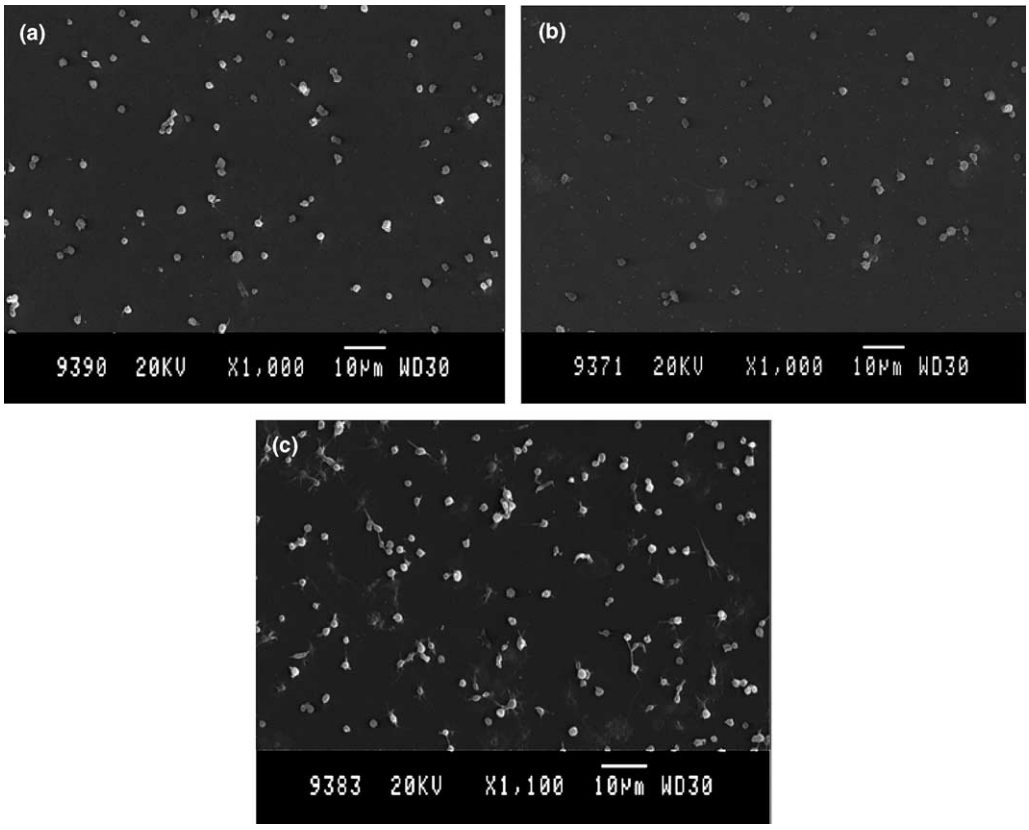

Fig. 3. SEM micrographs comparing the morphology and quantity of adherent platelets on: (a) untreated amorphous carbon, (b) N-PIII amorphous carbon and (c) LTIC.

for instance, adhesion quantity and morphology (shape), especially the aggregation and extent of pseudopodium. As shown in Fig. 3, the N-PIII a-C sample shows the least amount of adherent platelets that are also isolated and round indicating is very little destruction. In comparison, as shown in Fig. 3(c), most of the platelets on LTIC have undergone pseudopodium that is indicative of some activation. Further investigation indicates that there is an optimal argon to nitrogen flow ratio for best biocompatibility and it is related to graphitization of the materials [70].

Similarly, we have evaluated the blood compatibility of DLC doped with phosphorus. The synthesis of the DLC films and phosphorus implantation are again conducted in the same PIII&D machine with an evaporation source [72]. The Raman spectra obtained from the undoped and P-doped DLC are exhibited in Fig. 4. Two fitted Gaussian peaks are found at about 1530 cm^{-1} and

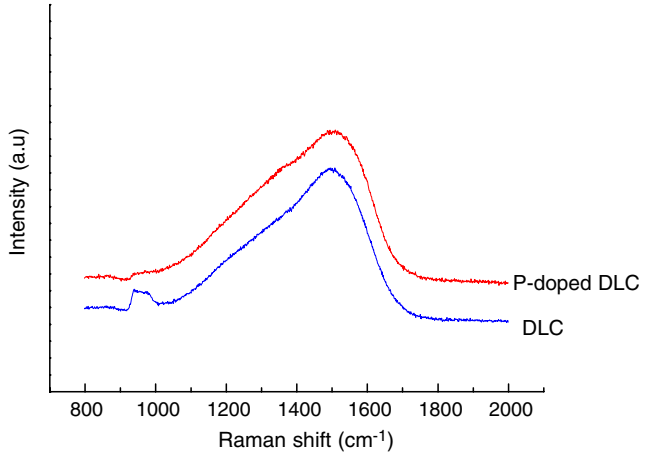

Fig. 4. Raman spectra acquired from the undoped a-C:H and phosphorus-doped DLC.

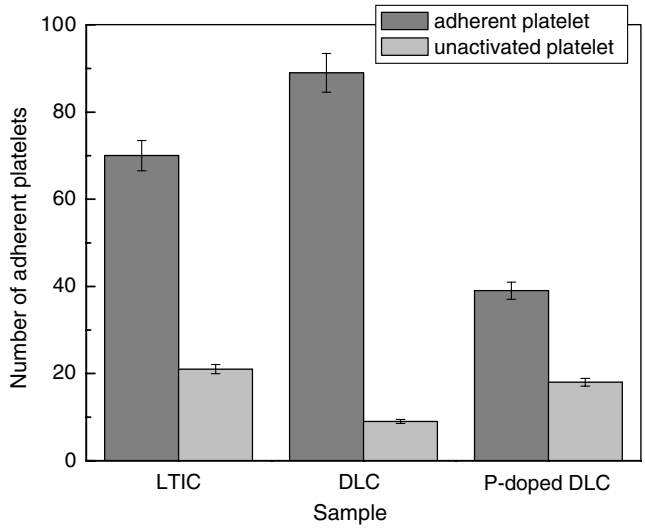

Fig. 5. Quantity of adherent platelets on LTIC, undoped DLC and P-doped DLC.

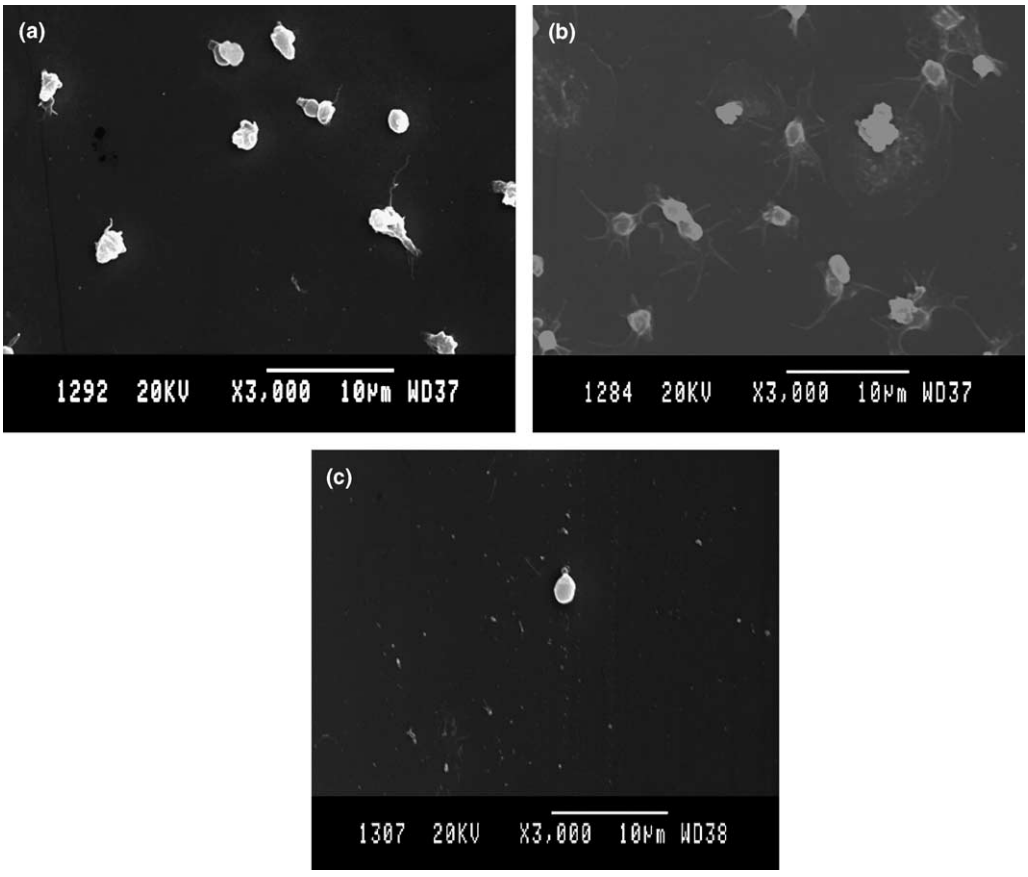

Fig. 6. Morphology of adherent platelets observed by SEM on (a) LTIC, (b) undoped DLC and (c) P-doped DLC.

1350 cm^{-1} corresponding to the G- and D-bands of graphite. For the P-doped DLC film, the full width at half maximum (FWHM) increases slightly whilst the G-band position shifts to 1520 cm^{-1}, suggesting a more disordered structure in the P-doped sample [73]. The platelet adhesion test shows significant difference in the behavior among the undoped and implanted materials. Fig. 5 displays the statistical amount of adherent platelets on LTIC, undoped DLC and P-doped DLC films after 20 min of incubation. An average of 39 contact-adherent platelets are observed on the P-doped DLC film, compared to 70 on the LTIC as a control. The highest number (89) of adhered platelets is found on the undoped DLC film. The morphology of adhered platelets is assessed using SEM. The platelets shape changes on the different surfaces after 120 min incubation are compared. The adherent platelets on the P-doped DLC (Fig. 6(c)) and LTIC (Fig. 6(a)) are isolated and relatively round. In comparison, most of the adherent platelets on the undoped DLC (Fig. 6(b)) are in aggregation exhibiting spreading pseudopodium.

5. Conclusion

Much progress has been made in the improvement of surface bioactivity of materials using plasma immersion ion implantation and deposition. This paper reviews the recent work conducted on the mitigation of Ni out-diffusion from NiTi shape memory alloys in orthopedic applications, enhancement of surface bioactivity of single-crystal silicon using hydrogen plasma implantation, as well as the improvement of blood compatibility of amorphous carbon using nitrogen and phosphorus plasma implantation.

Acknowledgments

The author thanks the members of the Plasma Laboratory as well as collaborators for their contributions. The work was jointly supported by Hong Kong Research Grants Council (RGC) Competitive Earmarked Research Grants (CERG) #CityU 1137/03E and #CityU 1120/04E, National Natural Science Foundation of China and Hong Kong Research Grants Council Joint Research Scheme project # N_CityU 101/03, as well as City University of Hong Kong Strategic Research Grant (SRG) #7001642.

References

[1] A. Anders (Ed.), Handbook of Plasma Immersion Ion Implantation and Deposition, John Wiley & Sons, New York, 2000.
[2] P.K. Chu, J.Y. Chen, L.P. Wang, N. Huang, Mater. Sci. Eng.: Rep. 36 (5–6) (2002) 143.
[3] P.K. Chu, J. Vac. Sci. Technol. 22 (1) (2004) 289.
[4] X.Y. Liu, R.W.Y. Poon, S.C.H. Kwok, P.K. Chu, C.X. Ding, Surf. Coat. Technol. 186 (1–2) (2004) 227.

[5] C.C. Shih, S.J. Lin, Y.L. Chen, Y.Y. Su, S.T. Lai, G.J. Wu, C.F. Kwok, K.H. Chung, J. Biomed. Mater. Res. 52 (2000) 395.
[6] M. Berger-Gorbet, B. Broxup, C. Rivard, L.H. Yahia, J. Biomed. Mater. Res. 32 (1996) 243.
[7] W. Jia, M.W. Beatty, R.A. Reinhardt, T.M. Petro, D.M. Cohen, C.R. Maze, E.A. Strom, M. Hoffman, J. Biomed. Mater. Res. 48 (1999) 488.
[8] L. Ponsonnet, V. Comte, A. Othmane, C. Lagneau, M. Charbonnier, M. Lissac, N. Jaffrezic, Mater. Sci. Eng. C 21 (2002) 157.
[9] A. Kapanen, J. Ilvesaro, A. Danilov, J. Ryhanen, P. Lehenkari, J. Tuukkanen, Biomaterials 23 (2002) 645.
[10] A. Kapanen, A. Kinnunen, J. Ryhanen, J. Tuukkanen, Biomaterials 23 (2002) 3341.
[11] L.B. Dalmau, H.C. Alberty, J.S. Parra, J. Prosthet. Dent. 52 (1984) 116.
[12] I.B. Lamster, D.I. Kalfus, P.J. Steigerwald, A.I. Chasens, J. Periodontol. 58 (1987) 486.
[13] W.E. Sanford, E. Niboer, in: E. Niboer, J.O. Nriagu (Eds.), Nickel and Human Health Current Perspectives, John Wiley & Sons, Canada, 1992, p. 123.
[14] A. Espana, M.L. Alonso, C. Soria, D. Guimaraens, A. Ledo, Contact Dermat. 21 (1989) 204.
[15] P.K. Chu, X.B. Tian, in: G.E. Totten, H. Liang (Eds.), Surface Modification and Mechanisms: Friction, Stress, and Reaction Engineering, Marcel Dekker, New York, 2004, p. 543 (Chapter 15).
[16] P.K. Chu, S. Qin, C. Chan, N.W. Cheung, L.A. Larson, Mater. Sci. Eng.: Rep. 17 (6–7) (1996) 207.
[17] P.K. Chu, Plasma Phys. Controlled Fusion 45 (5) (2003) 555.
[18] E. Mitura, A. Niedzielska, P. Niedzielski, L. Klimek, A. Rylski, S. Mitura, J. Moll, W. Pietrzykowski, Diamond Relat. Mater. 5 (1996) 998.
[19] S.K. Wu, C.Y. Lee, H.C. Lin, Scr. Mater. 37 (1997) 837.
[20] F. Vaz, P. Cerqueira, L. Rebouta, S.M.C. Nascimento, E. Alves, P. Goudeau, P. Rivière, K. Pischow, J. de Rijk, Thin Solid Films 447–448 (2004) 449.
[21] P.V. Kola, S. Daniels, D.C. Cameron, M.S.J. Hashmi, J. Mater. Process. Technol. 56 (1996) 422.
[22] S.A. Shabalovskaya, Bio. Med. Mater. Eng. 6 (1996) 267.
[23] L. Tan, Acta Mater. 50 (2002) 4449.
[24] S. Mändl, R. Sader, G. Thorwarth, D. Krause, H.F. Zeilhofer, H.H. Horch, B. Rauschenbach, Biomol. Eng. 19 (2002) 129.
[25] X. Nie, A. Leyland, A. Matthews, Surf. Coat. Technol. 125 (2000) 407.
[26] J.M. Lackner, W. Waldhauser, R. Ebner, B. Major, T. Schöberl, Surf. Coat. Technol. 180–181 (2004) 585.
[27] R.W.Y. Poon, K.W.K. Yeung, X.Y. Liu, P.K. Chu, C.Y. Chung, W.W. Lu, K.M.C. Cheung, D. Chan, Biomaterials 26 (15) (2005) 2265.
[28] R.W.Y. Poon, J.P.Y. Ho, X.Y. Liu, C.Y. Chung, P.K. Chu, K.W.K. Yeung, W.W. Lu, K.M.C. Cheung, Mater. Sci. Eng. A 390 (1–2) (2005) 444.
[29] X.B. Tian, R.K.Y. Fu, L.W. Wang, P.K. Chu, Mater. Sci. Eng. A 316 (2001) 200.
[30] R. Mientus, K. Ellmer, Surf. Coat. Technol. 116–119 (1999) 1093.
[31] K. Yokota, K. Nakamura, T. Kasuya, S. Tamura, T. Sugimoto, K. Akamatsu, K. Nakao, F. Miyashita, Surf. Coat. Technol. 158–159 (2002) 568.
[32] J.Y. Huang, L.L. Ye, Y.K. Wu, H.Q. Ye, Acta Mater. 44 (1996) 1781.
[33] A. Badzian, T. Badzian, Diamond Relat. Mater. 5 (1996) 93.
[34] L.L. Hench, O. Anderson, in: L.L. Hench, J. Wilson (Eds.), An Introduction to Bioceramics, World Scientific, USA, 1993, p. 41.
[35] P.N. De Aza, F. Guitian, S. De Aza, Scr. Mater. 31 (1994) 1001.
[36] X.Y. Liu, C.X. Ding, J. Biomed. Mater. Res. 59 (2) (2002) 259.
[37] X.Y. Liu, C.X. Ding, Biomaterials 22 (14) (2001) 2007.
[38] S. Cho, K. Nakanishi, T. Kokubo, N. Soga, J. Am. Ceram. Soc. 78 (1995) 1769.
[39] K.H. Karlsson, K. Fröberg, T.J. Ringbom, J. Non-Cryst. Solids 112 (1989) 69.
[40] E.M. Carlisle, in: D. Everd, M. O'Connor, et al. (Eds.), Silicon Biochemistry, John Wiley & Sons, Chichester, New York, Sydney, Toronto, Singapore, 1986, p. 123.
[41] M. Hidebrand, D.R. Higgins, K. Busser, B.E. Volcani, Gene 132 (1993) 213.
[42] L.L. Hench, Thermochim. Acta 280 (1996) 1.
[43] I.D. Xynos, M.V.J. Hukkanen, J.J. Batten, I.D. Buttery, L.L. Hench, J.M. Polak, Calcif. Tissue Int. 67 (2000) 321.
[44] I.D. Xynos, A.J. Edgar, L.D. Buttery, L.L. Hench, J.M. Polak, Biochem. Biophys. Res. Commun. 276 (2000) 461.
[45] J.W. Corbett, P. Deak, U.V. Desnica, S.J. Pearton, in: J.I. Pankove, N.M. Johnson (Eds.), Hydrogen in Semiconductors, Academic Press, San Diego, 1991, p. 49.
[46] Q.Y. Tong, U.M. Gösele, Adv. Mater. 11 (17) (1999) 1409.
[47] A. Piatkowska, G. Gawlik, J. Jagielski, Appl. Surf. Sci. 141 (1999) 333.
[48] J. Grisolia, F. Cristiano, G.B. Assayag, A. Claverie, Nucl. Instr. and Meth. B 178 (2001) 160.
[49] F.A. Reboredo, M. Ferconi, S.T. Pantelides, Phys. Rev. Lett. 82 (24) (1999) 4870.
[50] S.B. Zhang, W.B. Jackson, Phys. Rev. B 43 (14) (1991) 12142.
[51] H. Iwata, M. Takagi, Y. Tokuda, T. Imura, J. Cryst. Growth 210 (2000) 94.
[52] C. Dahmen, A. Janotta, D. Dimova-Malinovska, S. Marx, B. Jeschke, B. Nies, H. Kessler, M. Stutzmann, Thin Solid Films 427 (2003) 201.
[53] X.Y. Liu, R.K.Y. Fu, R.W.Y. Poon, P. Chen, P.K. Chu, C.X. Ding, Biomaterials 25 (2004) 5575.
[54] P.K. Chu, B.Y. Tang, Y.C. Cheng, P.K. Ko, Rev. Sci. Instr. 68 (1997) 1866.
[55] P.K. Chu, B.Y. Tang, L.P. Wang, X.F. Wang, S.Y. Wang, N. Huang, Rev. Sci. Instr. 72 (2001) 1660.
[56] Z.N. Fan, X.C. Zeng, D.T.K. Kwok, P.K. Chu, IEEE Trans. Plasma Sci. 28 (2000) 371.
[57] X.H. Wang, F. Zhang, C.R. Li, Z.H. Zheng, X. Wang, X.H. Liu, A.Q. Chen, Z.B. Jiang, Surf. Coat. Technol. 128–129 (2000) 36.
[58] F.Z. Cui, D.J. Li, Surf. Coat. Technol. 131 (2000) 481.
[59] A. Grill, Diamond Relat. Mater. 12 (2003) 166.
[60] S.E. Rodil, R. Olivares, H. Arzate, S. Muhl, Diamond Relat. Mater. 12 (2003) 931.
[61] J.Y. Chen, L.P. Wang, K.Y. Fu, N. Huang, Y. Leng, Y.X. Leng, P. Yang, J. Wang, G.J. Wan, H. Sun, X.B. Tian, P.K. Chu, Surf. Coat. Technol. 156 (2002) 289.
[62] P. Yang, S.C.H. Kwok, P.K. Chu, Y.X. Leng, J.Y. Chen, J. Wang, N. Huang, Nucl. Instr. and Meth. B 206 (2003) 721.
[63] Y.X. Leng, J.Y. Chen, P. Yang, H. Sun, G.J. Wan, N. Huang, Surf. Sci. 531 (2003) 177.
[64] D. Sheeja, B.K. Tay, L.N. Nung, Diamond Relat. Mater. 13 (2004) 184.
[65] R. Hauert, Diamond Relat. Mater. 12 (2003) 583.
[66] H. Inaba, S. Fujimaki, S. Sasaki, S. Hirano, S. Todoroki, K. Furusawa, M. Yamasaka, X. Shi, Jpn. J. Appl. Phys. 41 (2002) 5730.
[67] Y.Y. Chang, D.Y. Wang, W.T. Wu, Diamond Relat. Mater. 12 (2003) 2077.
[68] X.W. Zhang, N. Ke, W.Y. Cheung, S.P. Wong, Diamond Relat. Mater. 12 (2003) 1.
[69] P.Y. Tessier, L. Pichon, P. Villechaise, P. Linez, B. Angleraud, N. Mubumbila, V. Fouquet, A. Straboni, X. Milhet, H.F. Hildebrand, Diamond Relat. Mater. 12 (2003) 1233.
[70] S.C.H. Kwok, P. Yang, J. Wang, X.Y. Liu, P.K. Chu, J. Biomed. Mater. Res. A 70 (2004) 107.
[71] S.C.H. Kwok, J. Wang, P.K. Chu, Diamond Relat. Mater. 14 (1) (2005) 78.
[72] L.H. Li, R.W.Y. Poon, S.C.H. Kwok, P.K. Chu, Y.Q. Wu, Y.H. Zhang, Rev. Sci. Instr. 74 (10) (2003) 4301.
[73] M.T. Kuo, P.W. May, A. Gunn, M.N.R. Ashfold, R.K. Wild, Diamond Relat. Mater. 9 (2000) 1222.